ANTIOXIDANTS & REDOX SIGNALING
Volume 17, Number 4, 2012

DOI: 10.1089/ars.2011.4276

Insight into the Selenoproteome of the Malaria Parasite *Plasmodium falciparum*

Anne Röseler,[1] Judith Helena Prieto,[1] Rimma Iozef,[1] Beate Hecker,[1] Rolf Heiner Schirmer,[2] Simone Külzer,[3] Jude Przyborski,[3] Stefan Rahlfs,[1] and Katja Becker[1]

Abstract

Aims: The malaria parasite *Plasmodium falciparum* possesses four unique selenoproteins (*Pf*Sel1–*Pf*Sel4) which are likely to represent important components of the redox-regulatory network of this infectious agent. So far these proteins have only been characterized *in silico*. The aim of the present study was to gain further insight into the structural, biochemical, and functional properties of *P. falciparum* selenoproteins. ***Results:*** Using ^{75}Se labeling in *P. falciparum* cell culture, the presence of selenoproteins in the parasite could be verified for the first time. Bioinformatic analyses indicated distant relatedness between the *Plasmodium* proteins and selenoproteins described in other organisms, namely between *Pf*Sel1 and SelK, *Pf*Sel2 and SelT, and between *Pf*Sel4 and SelS. For *Pf*Sel3 no remarkable similarities with proteins from other organisms were identified. All four proteins were recombinantly produced in *Escherichia coli* as UGA→UGU (selenocysteine→cysteine) mutants. Using green fluorescent protein (GFP)-fusion proteins and immunofluorescence, the subcellular localization of the four selenoprotein mutants was studied. *Pf*Sel1, *Pf*Sel2, and *Pf*Sel4 localized to the endoplasmic reticulum whereas *Pf*Sel3 was visualized in the nucleus and/or the apicoplast. Functional assays support the roles of *Pf*Sel1 and *Pf*Sel4 in cellular redox reactions. Transcriptional profiles of the four selenoproteins, and proteins involved in selenoprotein biosynthesis, indicate that their expression is regulated *via* the availability of selenium and *via* oxidative and nitrosative stress. ***Innovation:*** In this study the presence of selenoproteins in *Plasmodium* has been proven for the first time; the subcellular localization of the proteins and their relatedness to known selenoproteins have been systematically studied, and recombinant proteins as well as information on regulation of transcript levels have been obtained. ***Conclusion:*** Taken together, our data enhance our understanding of the functional role of selenoproteins in *Plasmodium*. *Antioxid. Redox Signal.* 17, 534–543.

Introduction

Malaria is a threat to nearly 50% of the world's population. The World Health Organization estimated 225 million cases and 789,000 deaths in the year 2010 (40). The causative agents of malaria are parasites of the genus *Plasmodium*. The most severe form, *malaria tropica*, is caused by *Plasmodium falciparum*. Because of resistance to currently available drugs, there is an urgent need for new antimalarials and novel drug targets. Since the successful propagation of malaria parasites in their hosts depends on a balanced redox environment, interference with redox metabolism represents a promising strategy for antimalarial drug discovery (2, 3, 30).

Selenoproteins are selenocysteine (Sec)-containing proteins. Sec, the 21st genetically encoded amino acid, has a lower pKa and a higher reduction potential than cysteine, which

Innovation

In this study we prove for the first time the presence of selenoproteins in blood stages of the malaria parasite *P. falciparum*.

Detailed bioinformatic analyses indicate homologies between three of the *Plasmodium* proteins and selenoproteins described in other organisms. All four proteins were recombinantly produced and their subcellular localization was elucidated. Functional assays support the roles of *Pf*Sel1 and *Pf*Sel4 in cellular redox reactions. Transcriptional profiles of the four selenoproteins and of proteins involved in selenoprotein biosynthesis indicate that their expression is regulated by the availability of selenium and by oxidative and nitrosative stress. Taken together, the data enhance our understanding of the functional role of selenoproteins in *Plasmodium*.

[1]Interdisciplinary Research Center, Giessen University, Giessen, Germany.
[2]Biochemistry Centre, Heidelberg University, Heidelberg, Germany.
[3]Department of Parasitology, Faculty of Biology, Philipps University Marburg, Marburg, Germany.

makes the residue more reactive toward both electrophilic substrates and inhibitors (33). For Sec incorporation, the presence of selenium, a UGA codon (encoding Sec under the specific circumstances) and a Sec insertion sequence (SECIS) element, a conserved motif downstream of the selenoprotein encoding gene, are required (4, 15). A complex co-translational machinery then further assists the biosynthesis of selenoproteins (6, 8, 9, 11).

Selenoproteins are found in all 3 kingdoms of life, with about 30 different families currently identified (20). In humans there are 25 known selenoproteins (20). Among the best studied ones are glutathione peroxidases, thioredoxin reductases, and deiodinases (10, 14, 28, 31). Selenoproteins are key players in redox metabolism and in antioxidant defense. Moreover, proteins linked to redox metabolism—like thioredoxin glutathione reductase (21) and glucose-6-phosphate dehydrogenase (17)—are currently discussed as attractive antiparasitic drug targets (2, 3, 35).

We have previously identified the decoding machinery for selenoproteins and four unique possible genes of selenoproteins *via* computational analyses in *P. falciparum* (25). These four selenoproteins, namely *Pf*Sel1 (PF14_0033), *Pf*Sel2 (PFI1515w), *Pf*Sel3 (MAL8P1.86), and *Pf*Sel4 (PF14_0251) are highly conserved within *Plasmodium* species. *Pf*Sel1 and *Pf*Sel4 are relatively small with a molecular mass of 13.3 and 16.1 kDa, respectively. *Pf*Sel2 and *Pf*Sel3 have a molecular mass of 27.6 and 41.5 kDa, respectively (including predicted targeting sequences). The Sec residues are located in the C-terminal (*Pf*Sel1 and *Pf*Sel 4) or N-terminal (*Pf*Sel2 and *Pf*Sel3) regions of the proteins—some of them in direct vicinity to a cysteine residue (*Pf*Sel1 and *Pf*Sel2), which might be involved in enzymatic catalysis (25).

Within the framework of this present study, we aimed at enhancing our understanding of structural and functional properties of the four *P. falciparum* selenoproteins. Based on bioinformatic analyses, we propose similarities with selenoproteins from other organisms. Further, we heterologously overexpressed all four proteins as UGA→UGU (UGU corresponding to cysteine) mutants in *Escherichia coli* and additionally elucidated their subcellular localization in *Plasmodium* using green fluorescent protein (GFP) fusion proteins. Finally, we studied the influence of selenium, oxidative and nitrosative stress on transcript levels of the four selenoproteins which allows us first insights into regulatory processes.

Results

Selenium is incorporated into predicted plasmodial selenoproteins

By using ^{75}Se labeling in *P. falciparum* cell culture and evaluating the cell extract on an SDS gel by autoradiography, we detected five weak but distinct signals (Fig. 1). Bands were identified at molecular masses of about 16, 28, and 40 kDa, which correspond to the predicted molecular masses of *Pf*Sel4 (16.1 kDa), *Pf*Sel2 (27.6 kDa), and *Pf*Sel3 (41.5 kDa), respectively. Under the conditions chosen, a fourth signal around 50 kDa was detected which does not directly correspond to the predicted size of the identified selenoproteins, but which might represent an oligomer. A clear signal for *Pf*Sel1 at 13.3 kDa was not identified. However, the diffuse spot in the low molecular weight region of the gel might cover the respective band.

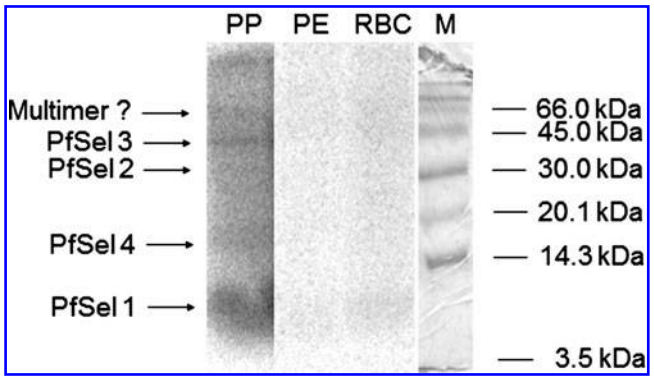

FIG. 1. Autoradiography of cell extract after 136 h incubation of *Plasmodium falciparum* blood stages with 1 μCi/ml $Na_2^{(75)}SeO_3$. Parasites were harvested in the trophozoite stage. Weak bands were identified at molecular masses of about 16, 28, and 40 kDa, which might correspond to the predicted molecular masses of *Pf*Sel4 (16.1 kDa), *Pf*Sel2 (27.6 kDa), and *Pf*Sel3 (41.5 kDa), respectively. A fourth signal around 50 kDa does not correspond to a predicted monomeric selenoprotein, however, might represent a selenoprotein oligomer. The rather diffuse signal in the low molecular weight region of the gel might cover the band of *Pf*Sel1 at 13.3 kDa. Although the bands detected are—due to low abundance of the proteins—rather faint, they represent the first *in vivo* proof of selenoproteins in *Plasmodium*. Despite varying concentrations of $Na_2^{(75)}SeO_3$, incubation times and parasite stages used for harvesting, the signals could not be improved. Se, selenium; Sel, selenoprotein; PP, parasite cell pellet; PE, parasite extract; RBC, red blood cell extract; M, marker proteins.

Bioinformatic analyses and heterologous overexpression

As discussed below, the sequences of all four predicted *Plasmodium* selenoproteins were studied in detail with various bioinformatics tools to identify homologous sequences and to further characterize structural motifs. Phylogenetic tree analysis was carried out with other predicted selenoproteins from related organisms. The results are given in the Supplementary Materials (*see* Supplementary Text and Figs. S1–S3; Supplementary Data are available online at www.liebertonline.com/ars).

Further we were able to clone and overexpress the genes of all four plasmodial selenoproteins as UGA→UGU (Sec→Cys) mutants in *E. coli*. However, the recombinant production turned out to be very challenging—with respect to yield, purity, and stability of the proteins—as described in detail in the Supplementary Methods and Results sections and in Supplementary Figure S4.

Pf*Sel1 and* Pf*Sel4 as "protector" proteins*

To study the general antioxidative activity of the selenoproteins, an assay system based on the protection of glutamine synthetase (GS) activity from oxidative stress induced by $FeCl_3$ and DTT was employed (19). Adding the iron chelator EDTA or a well-known peroxidase (in our case *P. falciparum* thioredoxin peroxidase 1 [TPx1]) to the assay system, protected the GS activity from inactivation; in case of *Pf*TPx1 this effect was concentration dependent (Fig. 2). A reproducible and concentration dependent protective activity was

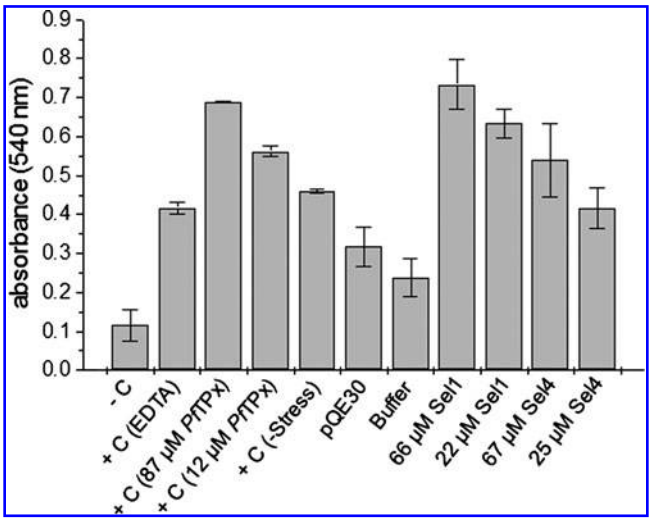

FIG. 2. Antioxidative activity of *Pf*Sel1 and *Pf*Sel4. The general antioxidative activity of the selenoproteins was examined using the glutamine synthetase protection assay according to Kim *et al.* (19). For these assays we employed the heterologously overexpressed and purified Sec→Cys mutants of the selenoproteins. −C: negative control, here GS is drastically inactivated by oxidative stress induced by $FeCl_3$ and DTT; +C (EDTA): in this positive control, the oxidative stress is diminished by the iron chelator EDTA; +C (87 or 12 μM *Pf*TPx): in these two positive controls, the oxidative stress is antagonized concentration-dependently by *P. falciparum* TPx1 (available as pure recombinant protein in our lab); +C (-Stress): in this positive control $FeCl_3$ was omitted; pQE30: negative control, *Escherichia coli* cell lysate with empty expression vector, purified *via* affinity chromatography as done for the selenoproteins; Buffer: negative control, only the 50 mM HEPES buffer (+TG-buffer) in which the selenoproteins were taken up was used; 66/22/67/25 μM Sel1 or Sel4: concentration dependent protective activity of *Pf*Sel1 and *Pf*Sel4. Sec, selenocysteine; TPx, thioredoxin peroxidase.

also found for *Pf*Sel1 and *Pf*Sel4, which were studied in the form of the recombinantly produced UGA→UGU mutants.

Subcellular localization of plasmodial selenoproteins

GFP-fusion proteins of the four plasmodial selenoproteins were expressed in *P. falciparum* with a UGA→UGU (cysteine) mutation replacing the Sec by a cysteine. For details on the design of the GFP fusion constructs and parasite transfection please refer to the Supplementary Material. It should be pointed out that a single amino acid exchange can theoretically alter the subcellular localization of a protein. Thus, the Cys mutants used in our studies cannot be ruled out to have other locations than the corresponding wild-type selenoproteins.

As shown in Figure 3, the cysteine mutants of three out of four selenoproteins, namely *Pf*Sel1, *Pf*Sel2, and *Pf*Sel4, localized reproducibly to the endoplasmic reticulum (ER).

However, the cysteine mutant of *Pf*Sel3 could not be clearly assigned to a defined compartment. Occasionally colocalization with apicoplast (Fig. 4A) and (in very few cases) with parasitophorous vacuole markers were detected (data not shown). The tryptophan mutant of *Pf*Sel3 clearly co-localized with the apicoplast marker acyl carrier protein (ACP) (Fig. 4B). The *Pf*Sel3-GFP fusion construct with the original Sec codon UGA (but without SECIS element) resulted in a strong nuclear localization as indicated by co-localization with the nuclear marker Hoechst 33258 (Fig. 4C). It will be interesting to study the observed phenomena in further detail.

Inhibition of P. falciparum *growth* in vitro

To determine the general growth promoting and inhibiting effects of selenite in *Plasmodium* and to define proper levels of selenite, paraquat, and sodium nitroprusside (SNP) for the following experiments on transcript level changes, the growth inhibitory effects of sodium selenite, paraquat, and SNP were determined *in vitro* in the *P. falciparum* K1 strain. The IC_{50} value of sodium selenite was determined to be 10.1 ± 3.2 μM which corresponds well with a recently published value of 9 μM (36). The IC_{50} values for SNP and paraquat were 8.8 ± 2.1 and 25 ± 4.8 μM, respectively. Dose response curves are shown in Figure 5.

Sodium selenite has an impact on selenoprotein transcription

To analyze the transcript levels of the selenoproteins after sodium selenite supplementation, we treated the parasite cell culture with three different concentrations: 0.1 and 1.5 μM, which represent human plasma concentrations (23), and 7 μM, which is nearly the IC_{50} of sodium selenite (see Fig. 5). Transcripts of arginyl-tRNA-synthetase (*atRNAsyn*) and glutaminyl-tRNA-synthetase were found to be most stable under the experimental conditions (see Materials and Methods) and were therefore used as internal reference genes. The transcription of the four selenoproteins was regulated differentially. Treatment with 0.1 and 1.5 μM sodium selenite induced at most time points an upregulation of the transcript levels of all four selenoproteins (Fig. 6). At 7 μM sodium selenite consistently downregulated the transcript levels of *PfSel2* (Fig. 6), whereas $PftRNA^{ser[sec]}$ was found to be upregulated by a factor of 2.5 at 3 h (data not shown).

Influence of oxidative and nitrosative stress on selenoprotein transcript levels

The influence of oxidative or nitrosative stress on the transcript levels of the selenoproteins was studied by exposing the parasite cultures to the redox cyclers methylene blue (MB) or paraquat or to the nitric oxide (NO)-donor SNP (please see also Materials and Methods and Fig. 5).

After MB exposure we identified lactate dehydrogenase (*LDH*) and glutaminyl-tRNA-synthetase (*gtRNAsyn*) as the best combination of internal reference genes and used them to normalize our data. After treatment of the parasites with MB only very moderate mRNA level changes of the plasmodial selenoproteins or of the biosynthesis machinery were detected (Table 1).

For the experiments with paraquat and SNP a combination of *18s rRNA* and seryl-tRNA-synthetase (*stRNAsyn*) transcript levels was most stable and used as a reference. Neither paraquat nor SNP dramatically changed the transcript levels of the selenoproteins. However, as seen in Table 1, SNP induced a downregulation of various transcript levels at 3 h including *PfSel2*, *PfSel3*, *PfSPS*, *PfEFSec*, and *PfSBP2*, whereas *PfSel1* and *PfSel4* were downregulated at 9 h. At 12 and 15 h, *PfSPS* and *PfSBP2* transcript levels increased—a trend that

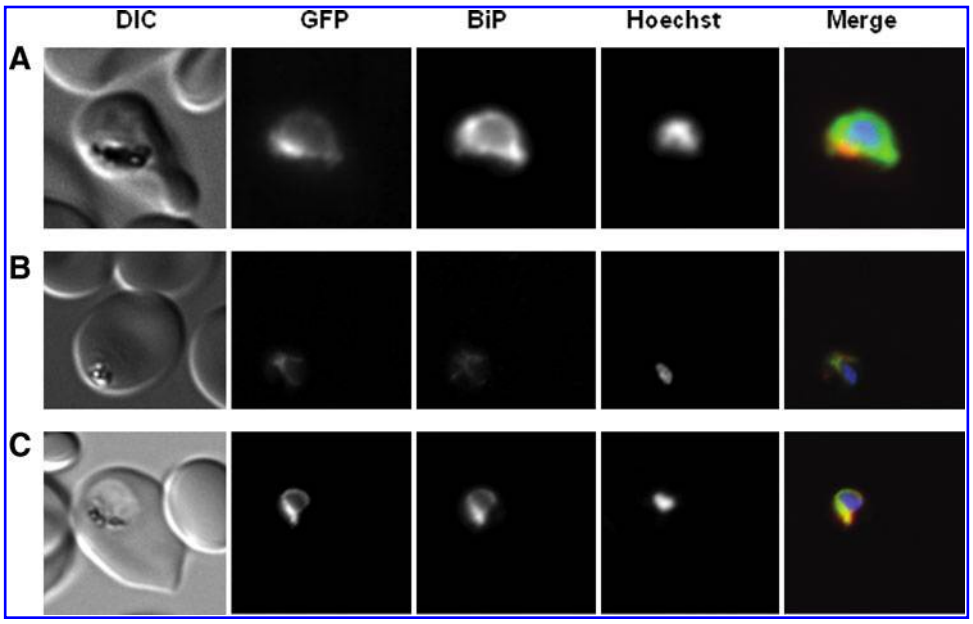

FIG. 3. Subcellular localization of *Pf*Sel1, *Pf*Sel2, and *Pf*Sel4 in *P. falciparum* using GFP-fusion proteins. Shown are erythrocytes infected with trophozoite stage parasites. **(A)** *Pf*Sel1 (Sec→Cys), **(B)** *Pf*Sel2 (Sec→Cys), and **(C)** *Pf*Sel4 (Sec→Cys). Anti-BiP and Hoechst 33258 were used for co-localization with endoplasmic reticulum and nucleus, respectively. DIC, differential interference contrast; GFP, green fluorescence protein; BiP, binding immunoglobulin protein. (To see this illustration in color the reader is referred to the web version of this article at www.liebertonline.com/ars).

was also seen under paraquat. In addition, supplementation of the parasite culture with paraquat led to slight decrease in the mRNA levels of *PfSel1* and *PfSel4* at 9 h—as also seen under SNP.

Discussion

Within the framework of this study, the occurrence of selenoproteins in the malaria parasite *P. falciparum* was definitely shown using ^{75}Se incorporation studies (Fig. 1). Further, structural, functional, and cell-biological properties of the four selenoproteins from this parasite have been determined. In the following we discuss these findings for each single protein (please see also Table 2 for a summary of the data).

Pf*Sel1, a SelK homologue*

As shown in Supplementary Figure S1, the primary structure of *Pf*Sel1 shares a similarity of 50.9% with human SelK, when comparing with *Toxoplasma gondii* SelK this value increases to 60.3%. Phylogenetic analyses indicate that the protein fits well into a predicted class of SelK proteins of protozoan parasites. The Sec residue of *Pf*Sel1 is found within a CxxxxUG redox motif similar to active site motifs found in other redox-active proteins. As demonstrated with GFP fusion proteins, the cysteine mutant of *Pf*Sel1 localizes to the ER (Fig. 3A), as it is also the case for human SelK (26). In both hSelK and *Pf*Sel1 sequences a transmembrane motif is predicted, however, in contrast to hSelK (20), no plasma

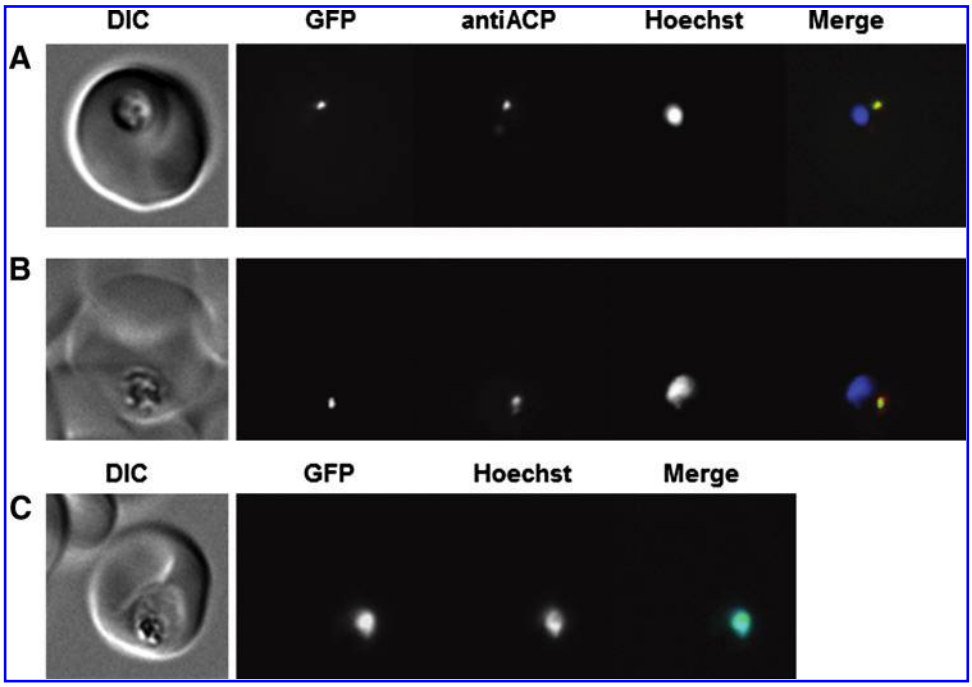

FIG. 4. Subcellular localization of *Pf*Sel3 in *P. falciparum* using GFP-fusion proteins and different *Pf*Sel3 mutants. Shown are erythrocytes infected with trophozoite stage parasites. **(A)** *Pf*Sel3 (Sec→Cys), **(B)** *Pf*Sel3 (Sec→Trp), and **(C)** *Pf*Sel3-UGA. Anti-ACP and Hoechst 33258 were used for co-localization with apicoplast and nucleus, respectively. ACP, acyl carrier protein. (To see this illustration in color the reader is referred to the web version of this article at www.liebertonline.com/ars).

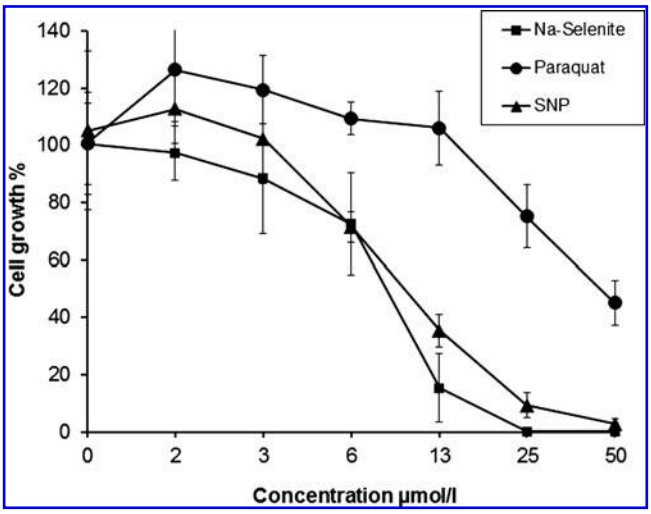

FIG. 5. Dose-response curves for sodium selenite, paraquat, and SNP on *P. falciparum* in cell culture. Parasites were grown as described in the Supplementary Materials. The experiments were carried out to determine the general growth promoting and inhibiting effects of selenite in *Plasmodium* and to define proper levels of selenite, paraquat, and SNP for the following experiments on transcript level changes. Please note that the drug concentrations given on the x-axis are nonlinear. SNP, sodium nitroprusside.

membrane localization was observed for our GFP-*Pf*Sel1 fusion protein.

In spite of the low yield of the recombinantly produced *Pf*Sel1, a concentration dependent antioxidant activity in the glutamine synthetase assay could be determined for *Pf*Sel1. Since for other selenoenzymes a Sec→Cys mutation shows an activity decrease of about 75%–99% (5, 7, 41), it is likely that the activity of native *Pf*Sel1 is much higher. Our findings are supported by the fact that for human SelK a decrease of reactive oxygen species levels was shown when the protein was overexpressed in cardiomyocytes (26).

*Pf*Sel1 mRNA levels decreased over time under high sodium selenite concentrations (Fig. 6) and hardly changed under oxidative or nitrosative stress (Table 1).

Pf*Sel2, a SelT homologue*

Alignments revealed 52.8% similarity between *Pf*Sel2 and human SelT (Supplementary Fig. S2) and also relatedness with SelT-like proteins from other organisms. Like in human SelT, in *Pf*Sel2 the Sec residue is found in a CxSU redox motif in the N-terminal section of the protein. Also for *Pf*Sel2 (Sec→Cys) an ER localization could be unambiguously demonstrated (Fig. 3B).

Determination of transcript levels indicated that *PfSel2* transcription depends on the selenium status in the parasite. In the presence of 0.1 and 1.5 μM sodium selenite *PfSel2* transcription increased within the first 3 h, whereas 7 μM sodium selenite consistently decreased the transcript level (0.3- to 0.7-fold) at all time points. In comparison with the other four selenoproteins, this phenomenon was very pronounced for *PfSel2*. Under oxidative or nitrosative stress no particular pattern of *PfSel2* transcript changes became evident—maybe with the exception of an initial slight downregulation under SNP and paraquat.

Interestingly, mammalian SelT was previously shown to play an important role in calcium homeostasis by mobilizing intracellular Ca^{2+} (13). In very preliminary analogously performed experiments an increase in cytosolic calcium levels was also detected when *Pf*Sel2 was overexpressed in *P. falciparum* (data not shown). This trend is likely to become much more pronounced if a Sec containing wild-type protein could be expressed. We aim at addressing this question in future studies once the difficulties in expression as for example, reported for human SelT in *E. coli* or yeast (10), can be technically handled.

Does Pf*Sel3 have a dual function in nucleus and apicoplast?*

Using several bioinformatic tools, no proteins with striking homologies to *Plasmodium* Sel3 were identified. However, a clear signal of about 40 kDa, corresponding to the predicted molecular mass of *Pf*Sel3 (41.5 kDa), was determined in the parasites after ^{75}Se supplementation. Interestingly, for *Pf*Sel3 a nuclear localization is predicted with a bipartite nucleus localization signal at the C-terminus (as 334–350). As described in the results section, the *Pf*Sel3/GFP-fusion protein, which contains its original UGA codon, indeed localized to the nucleus (Fig. 4C). UGA cannot be translated into Sec without the SECIS element, however, as described for other organisms, UGA might also code for cysteine or tryptophan (16, 27, 38). Therefore we produced *Pf*Sel3/GFP constructs with UGU (Cys) or UGG (Trp) instead of UGA. However, neither of these two mutants localized to the nucleus. The cysteine mutant localized in some cases to the apicoplast (Fig. 4A), in some cases to the parasitophorous vacuole and in most cases to indefinable compartments. The tryptophan mutant clearly localized to the apicoplast (Fig. 4B). These results might indicate that in *Plasmodium* UGA is unlikely to be translated to Cys or Trp in the absence of a SECIS element. It will be interesting to elucidate the mechanisms of this readthrough in further studies and to learn more about the physiological—and maybe dual—localization of wild-type *Pf*Sel3.

As determined in the real time polymerase chain reaction (rtPCR) experiments, the transcript levels of *PfSel3* quickly and strongly increased under 0.1 and 1.5 μM sodium selenite supplementation. A consistent or pronounced regulative pattern under oxidative or nitrosative stress was, however, not observed.

Based on the data, it is tempting to hypothesize that *Pf*Sel3 might serve as a sensor of selenium status possibly also influencing protein biosynthetic processes in the nucleus and the apicoplast.

Pf*Sel4 is a SelS homologue*

As for *Pf*Sel2 and *Pf*Sel3 we detected a 16 kDa signal corresponding to the predicted molecular mass of *Pf*Sel4 (16.1 kDa) in the ^{75}Se incorporation studies. Further, bioinformatic analyses revealed distant relatedness of *Pf*Sel4 with human SelS (Supplementary Fig. S3). The cysteine mutant of *Pf*Sel4 is located in the ER in *P. falciparum* (Fig. 3C) and—like human SelS—has a predicted transmembrane domain at positions 20–38.

Similar to *Pf*Sel1, we were able to overexpress small amounts of *Pf*Sel4 in *E. coli*. Optimizing the codon usage to *E. coli* by complete gene synthesis did not significantly improve the yield of the expression or the quality of the product. However, a general antioxidative activity of *Pf*Sel4 was demonstrated in the glutamine synthetase protection assay.

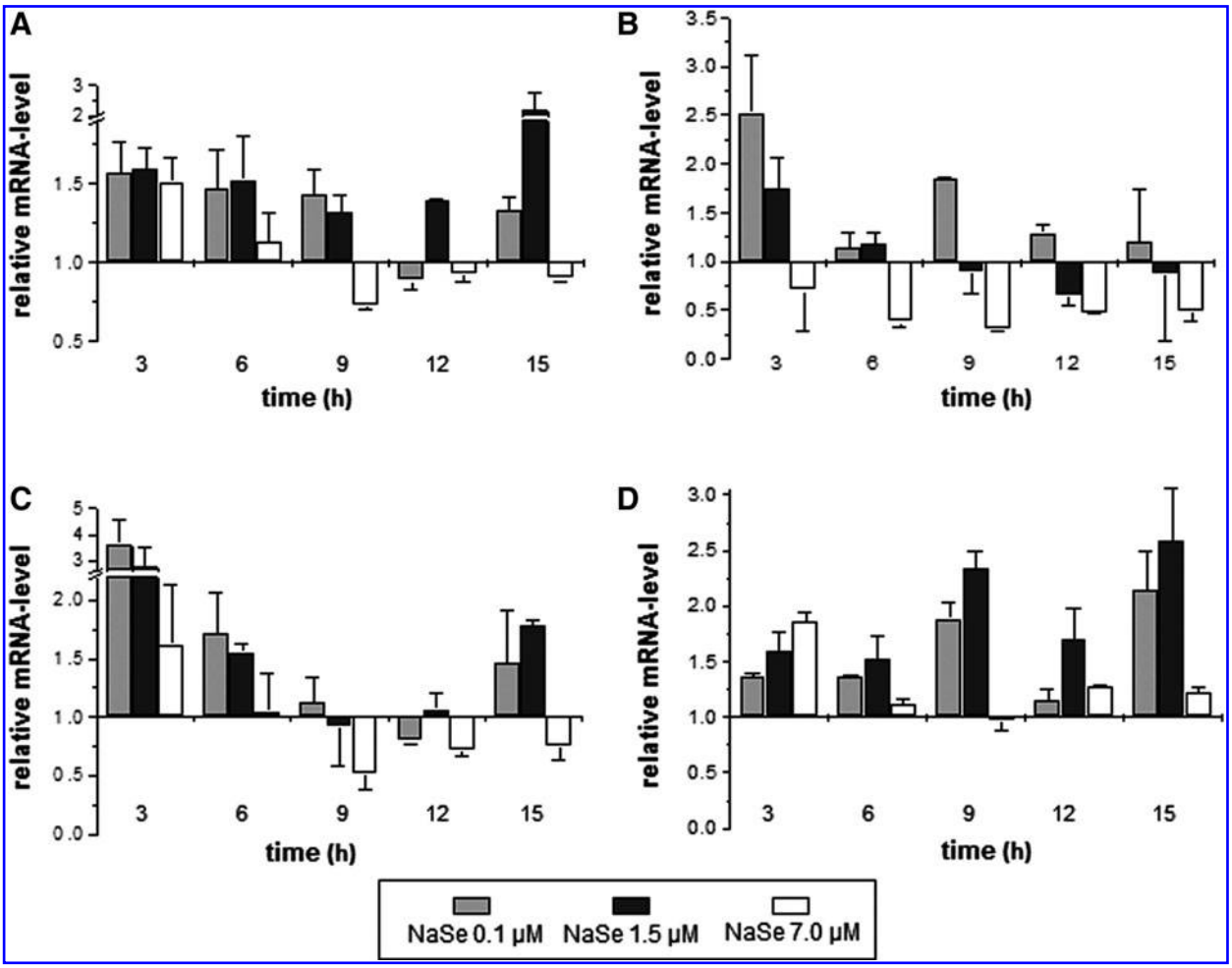

FIG. 6. mRNA levels of plasmodial selenoproteins are influenced by selenite status. Fifteen-hour-old ring-stage parasites were treated with three different sodium selenite concentrations (0.1, 1.5 and 7 μM). The parasites were harvested at 3, 6, 9, 12, and 15 h after addition of sodium selenite, RNA was isolated and transcript levels were determined as described in Materials and Methods and in the Supplementary Materials. Transcript changes relative to the untreated control were monitored for **(A)** *PfSel1*, **(B)** *PfSel2*, **(C)** *PfSel3*, and **(D)** *PfSel4*.

Transcript levels of *PfSel4* were enhanced at all time points under supplementation of the cell culture with 0.1 and 1.5 μM sodium selenite.

Selenoprotein biosynthesis machinery

The SECIS element works together with other *cis*- and *trans*-acting factors. Until now SECIS binding protein (SBP2), a specific $tRNA^{ser[sec]}$, a specific elongation factor (EFSec), Secp43, soluble liver antigen, ribosomal protein L30, nucleolin, Sec tRNA gene transcription activating factor, and Sec redefinition element have been identified to function for Sec insertion in eukaryotes (reviewed in 31). Numerous factors contributing to selenoprotein biosynthesis in *Plasmodium* have already been identified *in silico* (25) and were included into our studies on the regulation of transcript levels. Our data indicate that in *Plasmodium* the transcript levels of *SPS*, *EfSec* and $tRNA^{ser[sec]}$ are consistently upregulated by the presence of all three tested concentrations of sodium selenite over the period of 15 h (data not shown). In contrast, *SBP2* transcript levels increased at 3 h under all concentrations and decreased later. Under SNP and paraquat a clear increase in *SBP2*-transcript levels became evident at 12 and 15 h (Table 1).

The regulation of proteins involved in selenoprotein biosynthesis is likely to directly influence the gene expression of the four plasmodial selenoproteins. Such a hierarchical regulation of gene expression during different selenium statuses has been previously reported for mammals (32). Also regulatory pathways common to many selenoprotein genes, including several involved in stress-responses, have been proposed (11, 34). As recently published, such a stress response might even include selenium-induced apoptotic cell death in *Plasmodium* (36). Our data indicate that the factors contributing to transcription of selenoproteins in malaria parasites are directly regulated by sodium selenite and external stressors. Further studies will be carried out to elucidate the response of selenoprotein and selenoprotein synthesis genes to environmental and pharmacological challenges and to further understand the resulting adaptive processes in the parasites.

Table 1. Transcript Changes of *Plasmodium falciparum* Blood Stages Under Treatment with Methylene Blue, Sodium Nitroprusside, and Paraquat

	Ring		*Tropozoite*		*Schizont*
Gene	*3 h after treatment*	*6 h after treatment*	*9 h after treatment*	*12 h after treatment*	*15 h after treatment*
MB					
PfSel1	0.90 ± 0.03	2.09 ± 1.09	1.07 ± 0.49	0.72 ± 0.18	0.71 ± 0.04
PfSel2	1.66 ± 0.64	1.28 ± 0.25	1.30 ± 0.13	1.12 ± 0.08	1.57 ± 0.1
PfSel3	1.11 ± 0.59	1.17 ± 0.09	1.78 ± 0.59	1.32 ± 0.66	0.94 ± 0.07
PfSel4	0.52 ± 0.03	1.66 ± 0.37	1.23 ± 0.6	0.81 ± 0.14	0.66 ± 0.1
PfSPS	0.74 ± 0.23	1.51 ± 0.64	0.67 ± 0.11	1.07 ± 0.05	1.32 ± 0.21
PftRNA$^{ser[sec]}$	0.95 ± 0.09	2.32 ± 0.87	0.95 ± 0.36	1.21 ± 0.31	0.76 ± 0.01
PfEFSec	1.94 ± 1.13	1.56 ± 0.54	1.00 ± 0.18	1.31 ± 0.1	1.33 ± 0.63
PfSBP2	1.28 ± 0.37	1.08 ± 0.29	0.88 ± 0.18	2.22 ± 0.93	0.94 ± 0.18
SNP					
PfSel1	0.82 ± 0.27	0.8 ± 0.41	0.41 ± 0.03	1.29 ± 0.51	2.2 ± 1.07
PfSel2	0.16 ± n.a	1.71 ± n.a	1.38 ± n.a	0.37 ± n.a	3.58 ± n.a
PfSel3	0.28 ± 0.11	2.59 ± 1.91	0.47 ± 0.26	0.96 ± 0.33	1.26 ± 0.14
PfSel4	2.82 ± 2.38	0.7 ± 0.41	0.28 ± 0.16	0.73 ± 0.23	1.51 ± 0.15
PfSPS	0.23 ± 0.13	17.4 ± 17.2	0.9 ± 0.04	2.12 ± 1.48	4.37 ± 3.61
PftRNA$^{ser[sec]}$	2.61 ± 1.92	1.15 ± 0.1	0.55 ± 0.21	1.49 ± 0.17	1.6 ± 0.32
PfEFSec	0.42 ± 0.3	1.79 ± 0.68	0.67 ± 0.08	1.3 ± 0.04	1.19 ± 0.62
PfSBP2	0.37 ± n.a.	0.44 ± n.a.	0.16 ± n.a.	4.06 ± n.a.	19.22 ± n.a.
Paraquat					
PfSel1	1.82 ± 0.4	1.84 ± 0.55	0.47 ± 0.13	0.63 ± 0.29	2.56 ± 1.74
PfSel2	0.35 ± n.a	0.58 ± n.a	1.86 ± n.a	0.39 ± n.a	2.09 ± n.a
PfSel3	0.93 ± 0.16	0.9 ± 0.23	1.45 ± 0.90	2.45 ± 2.11	0.91 ± 0.39
PfSel4	1.77 ± 0.83	1.77 ± 0.67	0.31 ± 0.25	0.94 ± 0.45	1.69 ± 0.32
PfSPS	1.45 ± 0.79	3.48 ± 2.98	4.18 ± 0.51	0.77 ± 0.02	5.12 ± 4.34
PftRNA$^{ser[sec]}$	0.76 ± 0.03	1.09 ± 0.09	0.56 ± 0.25	1.61 ± 0.43	1.37 ± 0.69
PfEFSec	0.73 ± 0.14	1.17 ± 0.18	0.78 ± 0.06	1.12 ± 0.65	1.35 ± 0.56
PfSBP2	0.84 ± n.a	0.55 ± n.a	0.34 ± n.a	1.46 ± n.a	16.7 ± n.a

Given are relative mRNA concentration ± SE.

Fifteen-hour-old ring-stage parasites were treated with 10 μM SNP, 20 μM paraquat, or 15 nM MB. The parasites were harvested at 3, 6, 9, 12, and 15 h after addition of the compounds, RNA was isolated and transcript levels were determined as described in Materials and Methods and in the Supplementary Materials. Transcript changes relative to the untreated control were monitored.

MB, methylene blue; Se, selenium; Sel, selenoprotein; Sec, selenocysteine; SNP, sodium nitroprusside; n.a., not available.

Materials and Methods

^{75}Se incorporation studies

Parasites of the *P. falciparum* strain K1 were cultured as described in detail in Supplementary Material at a parasitemia of 8% and a hematocrit of 3.3%. Cultures of young ring stage parasites were continuously supplemented with 1 μCi/ml $Na_2{}^{(75)}SeO_3$ (Hartmann, Analytic GmbH) and grown for 136 h, which corresponds to two complete intraerythrocytic cyles of the parasite plus the growth phase from early rings to trophozoites (24). Harvesting was done in the trophozoite stage since here the yield in parasite material is highest. Shorter incubation times were tested but led to less ^{75}Se incorporation. After washing three times in saponin lysis buffer

Table 2. Summary of Properties of Selenoproteins in *Plasmodium falciparum*

	Pf*Sel1*	Pf*Sel2*	Pf*Sel3*	Pf*Sel4*
PlasmoDB ID	PF14_0033	PFI1515w	MAL8P1.86	PF14_0251
Chromosome	14	9	8	14
Size	13.3 kDa	27.6 kDa	41.5 kDa	16.1 kDa
Redox center	C-terminal	N-terminal	N-terminal	C-terminal
Vicinal cysteine	Yes	Yes	No	No
Homology	hSelK	hSelT	NA	hSelS
Subcellular localization	ER	ER	Nucleus* or Apicoplast *no SECIS element	ER
Putative function	Antioxidant	Hints toward involvement in Ca^{2+} homeostasis	Putative sensor for selenoprotein biosynthesis	Antioxidant
Influence on mRNA levels	NaSe↑*Pf*Sel1↓ O_2/NO *Pf*Sel1↔	NaSe↑*Pf*Sel2↑ NaSe↑↑ *Pf*Sel2↓ O_2/NO PfSel2↔	NaSe↑PfSel3↑↑ O_2/NO PfSel3↔	NaSe↑PfSel4↑

SECIS, Sec insertion sequence; NO, nitric oxide; ER, endoplasmic reticulum; NA, not applicable.

followed by centrifugation, parasites were disrupted by three cycles of freezing and thawing. Protein extracts were collected after centrifugation and separated by SDS-PAGE. The gel was dried and the ^{75}Se signals were visualized on an X-ray film.

Antioxidative activity

The general antioxidative activity of the selenoproteins was examined using the glutamine synthetase protection assay according to Kim *et al.* (19) For these assays we employed heterologously overexpressed and purified proteins (Sec→Cys mutants). *E. coli* cell extracts, grown with an empty expression vector, were used as controls.

Live cell imaging and immunofluorescence assays

Details on the design of GFP fusion constructs and parasite transfection are provided in the Supplementary Materials.

Immunofluorescence experiments were carried out either by fixing the cells with 4% paraformaldehyde/0.0075% glutaraldehyde in PBS of pH 7.4 as previously described (37) except that fixation was carried out for 30 min at 37°C, and quenching took place in 100 mM glycine/PBS. Primary antibodies used were the following: rabbit anti-ACP (1:500; kindly provided by GI McFadden), rabbit anti-BiP (1:2200; kindly provided by T. Gilberger), and chicken anti-GFP (1/1000; Abcam). Suitable Cy2- Cy3- (Dianova) conjugated secondary antibodies were used 1:2000. Antibodies were diluted in 3% bovine serum albumin-PBS. Fixed parasites were co-stained with Hoechst 33258 (50 ng/ml) to visualize nuclear DNA. Parasite cultures synchronized to about 80% were employed for the studies. Figures 3 and 4 show trophozoite stage parasites which are best suited for subcellular localization studies. Data shown are representative of at least 20 independent observations.

Determination of IC_{50}s on P. falciparum

Isotopic drug sensitivity assays were employed to investigate the susceptibility of the malaria parasites to various compounds. Incorporation of radioactive [^{3}H]hypoxanthine, was carried out with the modifications of Fivelman *et al.* (12) Parasites were incubated at a parasitemia of 0.25% (>70% ring forms) and 1.25% hematocrit in hypoxanthine-free medium. After 48 h, 0.5 μCi [^{3}H]hypoxanthine was added into each well, and the plates were incubated for another 24 h. The cells of each well were harvested on a glass fiber filter (Perkin-Elmer), washed, and dried. Their radioactivity, in counts per minute, was considered to be proportional to the respective growth of *P. falciparum* in the well. IC_{50} values were calculated.

Sample preparation for transcriptome profiling

Fifteen-hour-old ring-stage parasites were treated with 10 μM SNP, 20 μM paraquat, or 15 nM MB or three different sodium selenite concentrations (0.1, 1.5 and 7 μM). Culture conditions were chosen as described above. The parasites were harvested at 3, 6, 9, 12, and 15 h after treatment as described above. The parasites were frozen in liquid nitrogen and were kept at −80°C. For quantitative real-time-polymerase chain reaction (qR-T-PCR) the parasite cell extracts were prepared according to the instructions of the Macherey-Nagel NucleoSpin RNA/Protein kit with slight modifications. The pellet was resuspended in 350 μl RP-1 by carefully pipetting and at short vortexing intervals. Again 350 μl RP-1 was added to the suspension and the parasites were disrupted by three cycles of freezing in liquid N_2 and thawing in a water bath. Subsequently the RNA was purified according to the manufacturer's instruction.

Quantitative real-time PCR

For determining transcriptome changes two step quantitative real time PCR (qRT-PCR) was carried out after supplementation of the parasite cell culture with SNP, paraquat, sodium selenite, and MB.

Total RNA was isolated using the Macherey-Nagel NucleoSpin RNA/Protein kit as described above and treated with highly concentrated (1000 U) deoxyribonuclease I (Fermentas). RNA concentrations were measured by NanoDrop™ 1000 (ThermoScientific). Aliquots of 700 ng of each sample were reversely transcribed to cDNA using a 1:3 mix of oligo-dT and random hexamer primers (ThermoScientific Verso cDNA kit). The SYBR Green JumpStart Taq Ready Mix for Quantitative PCR (Sigma-Aldrich) or the SensiMix Sybr Kit (Bioline) was used with a Rotor-Gene 3000 real time PCR cycler (Corbett Research).

Primers were designed by hand or with FastPCR (18) Each primer was blasted against the whole *P. falciparum* genomic database to check for specificity and was also tested in a PCR prior to the qRT-PCR. The list of primers is shown in Supplementary Table S1. The qRT-PCR runs were performed in triplicates. Validations of the experiments were done by using freshly prepared cDNA. The Rotor-Gene 6.0 software was used to analyze the PCR results and to determine cycle threshold values.

18s rRNA, *LDH*, *atRNAsyn*, *gtRNAsyn*, *stRNAsyn* (22) served as internal reference genes. Normfinder (1) and GeNorm (39) were used to identify the most stable and best combination of two reference genes for every treatment. Relative mRNA-levels were calculated using the ΔΔ-CT-method (29).

Acknowledgments

The authors wish to thank the Deutsche Forschungsgemeinschaft for supporting the project (Be 1540/10-1 to KB and SFB 544, project B1 to HS). We thank Elisabeth Fischer for her excellent technical assistance in cell culture as well as Raphael Eberle and Maike Eisenkolb for their experimental support and helpful discussions.

Author Disclosure Statement

No competing financial interests exist.

References

1. Andersen CL, Jensen JL, and Orntoft TF. Normalization of real-time quantitative reverse transcription-PCR data: a model-based variance estimation approach to identify genes suited for normalization, applied to bladder and colon cancer data sets. *Cancer Res* 64: 5245–5250, 2004.
2. Becker K. *Apicomplexan Parasites: Molecular Approaches Toward Targeted Drug Development*. Weinheim: Wiley-Blackwell, 2011, xxi, p. 528.
3. Becker K, Tilley L, Vennerstrom JL, Roberts D, Rogerson S, and Ginsburg H. Oxidative stress in malaria parasite-infected erythrocytes: host-parasite interactions. *Int J Parasitol* 34: 163–189, 2004.

4. Berry MJ, Banu L, Harney JW, and Larsen PR. Functional characterization of the eukaryotic SECIS elements which direct selenocysteine insertion at UGA codons. *EMBO J* 12: 3315–3322, 1993.
5. Berry MJ, Maia AL, Kieffer JD, Harney JW, and Larsen PR. Substitution of cysteine for selenocysteine in type I iodothyronine deiodinase reduces the catalytic efficiency of the protein but enhances its translation. *Endocrinology* 131: 1848–1852, 1992.
6. Bock A. Biosynthesis of selenoproteins—an overview. *Biofactors* 11: 77–78, 2000.
7. Buettner C, Harney JW, and Larsen PR. The role of selenocysteine 133 in catalysis by the human type 2 iodothyronine deiodinase. *Endocrinology* 141: 4606–4612, 2000.
8. Caban K and Copeland PR. Size matters: a view of selenocysteine incorporation from the ribosome. *Cell Mol Life Sci* 63: 73–81, 2006.
9. Cassago A, Rodrigues EM, Prieto EL, Gaston KW, Alfonzo JD, Iribar MP, Berry MJ, Cruz AK, and Thiemann OH. Identification of *Leishmania* selenoproteins and SECIS element. *Molecular and Biochemical Parasitology* 149: 128–134, 2006.
10. Dikiy A, Novoselov SV, Fomenko DE, Sengupta A, Carlson BA, Cerny RL, Ginalski K, Grishin NV, Hatfield DL, and Gladyshev VN. SelT, SelW, SelH, and Rdx12: genomics and molecular insights into the functions of selenoproteins of a novel thioredoxin-like family. *Biochemistry* 46: 6871–6882, 2007.
11. Driscoll DM and Copeland PR. Mechanism and regulation of selenoprotein synthesis. *Annu Rev Nutr* 23: 17–40, 2003.
12. Fivelman QL, Adagu IS, and Warhurst DC. Modified fixed-ratio isobologram method for studying *in vitro* interactions between atovaquone and proguanil or dihydroartemisinin against drug-resistant strains of Plasmodium falciparum. *Antimicrob Agents Chemother* 48: 4097–4102, 2004.
13. Grumolato L, Ghzili H, Montero-Hadjadje M, Gasman S, Lesage J, Tanguy Y, Galas L, Ait-Ali D, Leprince J, Guerineau NC, Elkahloun AG, Fournier A, Vieau D, Vaudry H, and Anouar Y. Selenoprotein T is a PACAP-regulated gene involved in intracellular Ca2+ mobilization and neuroendocrine secretion. *FASEB J* 22: 1756–1768, 2008.
14. Hawkes WC and Alkan Z. Regulation of redox signaling by selenoproteins. *Biol Trace Elem Res* 134: 235–251, 2010.
15. Hill KE, Lloyd RS, and Burk RF. Conserved nucleotide sequences in the open reading frame and 3′ untranslated region of selenoprotein P mRNA. *Proc Natl Acad Sci U S A* 90: 537–541, 1993.
16. Inamine JM, Ho KC, Loechel S, and Hu PC. Evidence that UGA is read as a tryptophan codon rather than as a stop codon by Mycoplasma pneumoniae, Mycoplasma genitalium, and Mycoplasma gallisepticum. *J Bacteriol* 172: 504–506, 1990.
17. Jortzik E, Mailu BM, Preuss J, Fischer M, Bode L, Rahlfs S, and Becker K. Glucose-6-phosphate dehydrogenase-6-phosphogluconolactonase: a unique bifunctional enzyme from Plasmodium falciparum. *Biochem J* 436: 641–650, 2011.
18. Kalendar R, Lee D, and Schulman AH. FastPCR software for PCR primer and probe design and repeat search. *Genes, Genomes and Genomics* 3: 1–14, 2009.
19. Kim K, Kim IH, Lee KY, Rhee SG, and Stadtman ER. The isolation and purification of a specific "protector" protein which inhibits enzyme inactivation by a thiol/Fe(III)/O2 mixed-function oxidation system. *J Biol Chem* 263: 4704–4711, 1988.
20. Kryukov GV, Castellano S, Novoselov SV, Lobanov AV, Zehtab O, Guigo R, and Gladyshev VN. Characterization of mammalian selenoproteomes. *Science* 300: 1439–1443, 2003.
21. Kuntz AN, Davioud-Charvet E, Sayed AA, Califf LL, Dessolin J, Arner ES, and Williams DL. Thioredoxin glutathione reductase from Schistosoma mansoni: an essential parasite enzyme and a key drug target. *PLoS Med* 4: e206, 2007.
22. Lavazec C, Sanyal S, and Templeton TJ. Hypervariability within the Rifin, Stevor and Pfmc-2TM superfamilies in Plasmodium falciparum. *Nucleic Acids Res* 34: 6696–6707, 2006.
23. Levander OA. A global view of human selenium nutrition. *Annu Rev Nutr* 7: 227–250, 1987.
24. Liu Q, Lauridsen E, and Clausen J. Different selenium-containing proteins in the extracellular and intracellular media of leucocytes cultivated *in vitro*. *Biol Trace Elem Res* 61: 237–252, 1998.
25. Lobanov AV, Delgado C, Rahlfs S, Novoselov SV, Kryukov GV, Gromer S, Hatfield DL, Becker K, and Gladyshev VN. The Plasmodium selenoproteome. *Nucleic Acids Res* 34: 496–505, 2006.
26. Lu C, Qiu F, Zhou H, Peng Y, Hao W, Xu J, Yuan J, Wang S, Qiang B, Xu C, and Peng X. Identification and characterization of selenoprotein K: an antioxidant in cardiomyocytes. *FEBS Lett* 580: 5189–5197, 2006.
27. Macino G, Coruzzi G, Nobrega FG, Li M, and Tzagoloff A. Use of the UGA terminator as a tryptophan codon in yeast mitochondria. *Proc Natl Acad Sci U S A* 76: 3784–3785, 1979.
28. Papp LV, Holmgren A, and Khanna KK. Selenium and selenoproteins in health and disease. *Antioxid Redox Signal* 12: 793–795, 2010.
29. Pfaffl MW. A new mathematical model for relative quantification in real-time RT-PCR. *Nucleic Acids Res* 29: e45, 2001.
30. Prast-Nielsen S, Huang HH, and Williams DL. Thioredoxin-glutathione reductase: Its role in redox biology and potential as a target for drugs against neglected diseases. *Biochim Biophys Acta* 1810: 1262–1271, 2011.
31. Reeves MA and Hoffmann PR. The human selenoproteome: recent insights into functions and regulation. *Cell Mol Life Sci* 66: 2457–2478, 2009.
32. Schomburg L and Schweizer U. Hierarchical regulation of selenoprotein expression and sex-specific effects of selenium. *Biochim Biophys Acta* 1790: 1453–1462, 2009.
33. Stadtman TC. Selenocysteine. *Annu Rev Biochem* 65: 83–100, 1996.
34. Stoytcheva ZR and Berry MJ. Transcriptional regulation of mammalian selenoprotein expression. *Biochim Biophys Acta* 1790: 1429–1440, 2009.
35. Sturm N, Jortzik E, Mailu BM, Koncarevic S, Deponte M, Forchhammer K, Rahlfs S, and Becker K. Identification of proteins targeted by the thioredoxin superfamily in Plasmodium falciparum. *PLoS Pathog* 5: e1000383, 2009.
36. Suradji EW, Hatabu T, Kobayashi K, Yamazaki C, Abdulah R, Nakazawa M, Nakajima-Shimada J, and Koyama H. Selenium-induced apoptosis-like cell death in Plasmodium falciparum. *Parasitology* 19: 1–11, 2011.
37. Tonkin CJ, van Dooren GG, Spurck TP, Struck NS, Good RT, Handman E, Cowman AF, and McFadden GI. Localization of organellar proteins in Plasmodium falciparum using a novel set of transfection vectors and a new immunofluorescence fixation method. *Mol Biochem Parasitol* 137: 13–21, 2004.
38. Turanov AA, Lobanov AV, Fomenko DE, Morrison HG, Sogin ML, Klobutcher LA, Hatfield DL, and Gladyshev VN. Genetic code supports targeted insertion of two amino acids by one codon. *Science* 323: 259–261, 2009.
39. Vandesompele J, De Preter K, Pattyn F, Poppe B, Van Roy N, De Paepe A, and Speleman F. Accurate normalization of real-time quantitative RT-PCR data by geometric averaging

of multiple internal control genes. *Genome Biol* 3: RESEARCH0034, 2002.
40. WHO. *World Malaria Report 2010*. Available at www.who.int/malaria/world_malaria_report_2010/worldmalariareport2010.pdf. 2010 Accessed on October 12, 2011.
41. Zhong L and Holmgren A. Essential role of selenium in the catalytic activities of mammalian thioredoxin reductase revealed by characterization of recombinant enzymes with selenocysteine mutations. *J Biol Chem* 275: 18121–18128, 2000.

Address correspondence to:
Dr. Katja Becker
Chair of Biochemistry and Molecular Biology
Interdisciplinary Research Center
Giessen University
Heinrich-Buff-Ring 26–32
35392 Giessen
Germany

E-mail: katja.becker@uni-giessen.de

Date of first submission to ARS Central, September 9, 2011; date of final revised submission, January 9, 2012; date of acceptance, January 9, 2012.

Abbreviations Used

ACP = acyl carrier protein
atRNAsyn = arginyl-tRNA-synthetase
ER = endoplasmic reticulum
GFP = green fluorescence protein
GS = glutamine synthetase
gtRNAsyn = glutaminyl-tRNA-synthetase
LB = Luria-Bertani
LDH = lactate dehydrogenase
MB = methylene blue
NLS = nucleus localization signals
NO = nitric oxide
qRT-PCR = quantitative real time PCR
RBC = red blood cell
RT-PCR = real time polymerase chain reaction
Sec = selenocysteine
SECIS = Sec insertion sequence
Sel = selenoprotein
SNP = sodium nitroprusside
stRNAsyn = seryl-tRNA-synthetase
TB = Terrific Broth
TPx = thioredoxin peroxidase